Oral presentation | Fluid-structure interaction

Fluid-structure interaction-II

Mon. Jul 15, 2024 2:00 PM - 4:00 PM Room A

[2-A-02] Development of an Elastic-Plastic Eulerian Solver for High-Speed Deformations with the Johnson-Cook Material Model

*Oren Peles[1], Moran Ezra[1], Marcel Martins Alves[1], Yoram Kozak[1], Nitsan Briskin[2], Avi Uzi[2], David Touati[2], Sharon Peles[2] （1. Tel-Aviv University, 2. Elbit Systems Land）

Keywords: Elastic-Plastic flow eulerian solver, Ghost fluid method, multi-material, level-set method, conjugate fluid-elastic-plastic

Development of an Elastic-Plastic Eulerian Solver for High-Speed Deformations with the Johnson-Cook Material Model

Oren Peles[1], Moran Ezra[1], Marcel Martins Alves[1], Nitsan Briskin[2], Sharon Peles[2], Avi Uzi[2], David Touati[2], Yoram Kozak[1]

[1]Combustion AND Energy Lab (CANDEL)
School of Mechanical Engineering, Tel Aviv University, Israel
[2]Elbit Systems, Israel

Twelfth International Conference on
Computational Fluid Dynamics (ICCFD12), July 2024

Lecture outline

Picture: car crash test from https://www.globalncap.org/

Introduction

- Elastic-plastic deformations arise when strong external forces are acting on the surfaces of elastic-plastic materials for example during high-speed impact or penetration events.
- These problems can be described by a set of hyperbolic equations that are similar to the compressible Euler equations for fluids.
- During the impact, the body is deforming; hence, its boundary is moving, which leads to a free-surface problem.
- The material can evolve from elastic to plastic state and vice versa. Hence, criterion for this transition should be applied.
- In the elastic regime, two types of waves exist - acoustic waves and transverse shear waves. In the plastic regime, only acoustic waves exist.

Our code Athena-RFX++

- Based on the open-source astrophysical code Athena++
- Fully compressible flow solver
- High-order Godunov method
- Euler or Navier-Stokes equations
- Heat and mass transfer diffusive processes and scalar advection
- Static and Adaptive Mesh Refinement (AMR)
- Excellent parallel scalability
- In-house developed numerical capabilities - Immersed boundary method for complex geometries and Level-set with Ghost fluid method for deforming bodies.

Wilkins model equations for Elastic-plastic deformation

- In the elastic state the model equations are [W+63]:

$$\frac{\partial \rho}{\partial t} + \nabla\left(\rho \vec{u}\right) = 0$$
$$\frac{\partial \rho \vec{u}}{\partial t} + \nabla\left(\rho \vec{u} \otimes \vec{u} - \sigma\right) = 0$$
$$\frac{\partial \rho E}{\partial t} + \nabla\left(\rho E \vec{u} - \sigma \cdot \vec{u}\right) = 0$$
$$\frac{\partial \rho S}{\partial t} + \nabla\left(\rho S \vec{u}\right) = 2\rho G\left(D - \frac{1}{3} Tr(D) I\right)$$

- where $\sigma = S - pI$ is Cauchy stress tensor, D is the strain tensor, S is the deviatoric stress, G is the shear modulus.
- The total energy is given by $E = e + \frac{1}{2}\left|\vec{u}\right|^2$ where e is the internal energy. Here, we consider the Mie-Grüneisen EOS: $p = \rho_0 a_0^2 f(\rho) + \rho_0 \Gamma_0 e$

- For the elastic state, the acoustic speed of sound is given by

$$c_a = \sqrt{a^2 + \frac{4}{3}\frac{G}{\rho}}$$

where

$$a^2 = a_0^2 \rho_0 \frac{df}{d\rho} + \frac{p\rho_0}{\rho^2}\Gamma_0$$

The speed of the slow shear wave is

$$c_s = \sqrt{\frac{G}{\rho}}$$

Plastic state

- In the plastic state, the equation for the stress tensor is given by

$$\frac{\partial \rho S}{\partial t} + \nabla\left(\rho S \vec{u}\right) = 2\rho G\left(D - \frac{1}{3}tr(D)I - D_p\right)$$

where D_p is the plastic strain tensor given by

$$D_p = -\frac{S}{\|S\|}\Lambda \qquad (1)$$

where Λ is a constant.

- $\|S\| = \sqrt{\frac{2}{3}}\|S_e\| = \sqrt{\frac{2}{3}}\sigma_y\left(\varepsilon_p, \frac{d\varepsilon_p}{dt}, T\right)$
where ε_p is the plastic strain, T is the temperature, σ_y is the yield stress, in Johnson-Cook material model given by

$$\sigma_y = \left(A + B\varepsilon_p^n\right)\left(1 + C\ln\frac{d\varepsilon_p}{dt}\right)\left(1 - \left(\frac{T-T_r}{T_m-T_r}\right)^m\right)$$

where A, B, C are constants, T_r is a reference temperature and T_m is the melting temperature.

- We also need to solve equations for the temperature and the plastic strain:

$$\frac{\partial \varepsilon_p}{\partial t} + \vec{u}\nabla\varepsilon_p = \Lambda \tag{2}$$

$$\frac{\partial T}{\partial t} + \vec{u}\nabla T = \alpha\nabla^2 T + \frac{\eta \|S\|}{\rho C_p}\Lambda \tag{3}$$

- The transition between elastic and plastic states (von Mises criterion) occurs when

$$\|S_e\| \geqslant \sigma_y\left(\varepsilon_p, \frac{d\varepsilon_p}{dt}, T\right)$$

- Once the material is at plastic state, we need to ensure that $\|S_e\| = \sigma_y$. This procedure is called radial remapping.

Radial remapping algorithm - Standard approach

- The transition from elastic to plastic states is splitted to an elastic predictor step (with $D_p = 0$) and a plastic correction step.
- In the plastic correction step, the equation for the deviatoric stress, is given by

$$\frac{dS}{dt} = -2GD_p. \tag{4}$$

- At the end of the plastic correction step $\left\|S_e^{n+1}\right\| = \sigma_y^{n+1}$.

- Using the relation $\triangle\varepsilon_p \approx \Lambda\triangle t$, integrating (4) for one time step with $S(0) = S^{tr}$ yields

$$S^{n+1} = S^{tr} - 2G\frac{\Lambda S^{tr}}{\|S^{tr}\|}\triangle t = S^{tr} - 2G\frac{S^{tr}}{\|S^{tr}\|}\triangle\varepsilon_p \tag{5}$$

Hence,

$$\left\|S_e^{(n+1)}\right\| = \sigma_y^{n+1}\left(\varepsilon_p + \Delta\varepsilon_p, \frac{\Delta\varepsilon_p}{\Delta t}, T + \Delta T\right) \tag{6}$$

where

$$\Delta T = \frac{\eta}{\rho C_p}\|S\|\,\Delta\varepsilon_p$$

and the approximation $\dot{\varepsilon}_p \approx \frac{\Delta\varepsilon_p}{\Delta t}$ is used.
- Equation (6) is a nonlinear equation for $\Delta\varepsilon_p$ that can be solved iteratively, for instance, via the Newton-Raphson method.
- After $\Delta\varepsilon_p$ is evaluated, the new temperature, stress tensor, and plastic strain can be evaluated.

New approach

- With the purpose of avoiding the need of solving a non-linear algebraic equation, we propose a different approach
- We consider the splitting between the elastic predictor and the plastic corrector as a true operator splitting where the plastic step with constrain $\|S\| = \sqrt{\frac{2}{3}}\sigma_y$ represents a differential-algebraic equation (DAE) problem that has to be solved where the DAE for ε_p is given by

$$F(S, \varepsilon_p, \dot{\varepsilon}_p, T) = \|S\| - \sqrt{\frac{2}{3}}\sigma_y(\varepsilon_p, \dot{\varepsilon}_p, T) = 0 \tag{7}$$

Coupled to the equations for S, T and ε_p.
- A first-order temporal approximation of Eq. (7) is:

$$\|S_e^{n+1}\| = \sigma_y^{n+1} \approx \sigma_y^{tr} + h\Delta\varepsilon_p - \frac{\partial\sigma_y}{\partial\dot{\varepsilon}_p}\dot{\varepsilon}_p^n \tag{8}$$

where

$$h \equiv \frac{d\sigma_y}{d\varepsilon_p} + \frac{\partial \sigma_y}{\partial T}\frac{dT}{d\varepsilon_p} + \frac{\partial \sigma_y}{\partial \dot{\varepsilon}_p}\frac{1}{\Delta t}$$

- Using the following approximations

$$\Delta\varepsilon_p = \varepsilon^{(n+1)} - \varepsilon^{(n)} = \dot{\varepsilon}_p \Delta t$$

and

$$\Delta\dot{\varepsilon}_p = \dot{\varepsilon}_p^{n+1} - \dot{\varepsilon}_p^{n} = \frac{\Delta\varepsilon_p}{\Delta t} - \dot{\varepsilon}_p^{n}$$

and substitution of S^{n+1} from Eq. (5) into Eq. (8) including some algebraic steps yields an equation for $\Delta\varepsilon_p$:

$$\Delta\varepsilon_p = \sqrt{\frac{2}{3}}\frac{\|S^{tr}\| - \sqrt{\frac{2}{3}}\left(\sigma_y - \frac{\partial \sigma_y}{\partial \dot{\varepsilon}_p}\dot{\varepsilon}_p^{n}\right)}{2G\left(1 + \frac{h}{3G}\right)}$$

Verification of JC algorithm

- We suggest a simplified zero-dimensional model for convergence and order of accuracy tests of our newly proposed algorithm for time splitting between the elastic and plastic state.
- In the elastic step, we solve for scalar stress S, temperature, and plastic strain, the equations with constant strain rate, D:

$$\frac{dS}{dt} = 2GD$$
$$\frac{dT}{dt} = 0$$
$$\frac{d\varepsilon_p}{dt} = 0.$$

- The simplified plastic transition condition is given by

$$S \geqslant \sigma_y\left(\varepsilon_p, \frac{d\varepsilon_p}{dt}, T\right).$$

Comparison of our numerical simulations of the simplified 0D model against experimental data (cross marks) from [JC85].

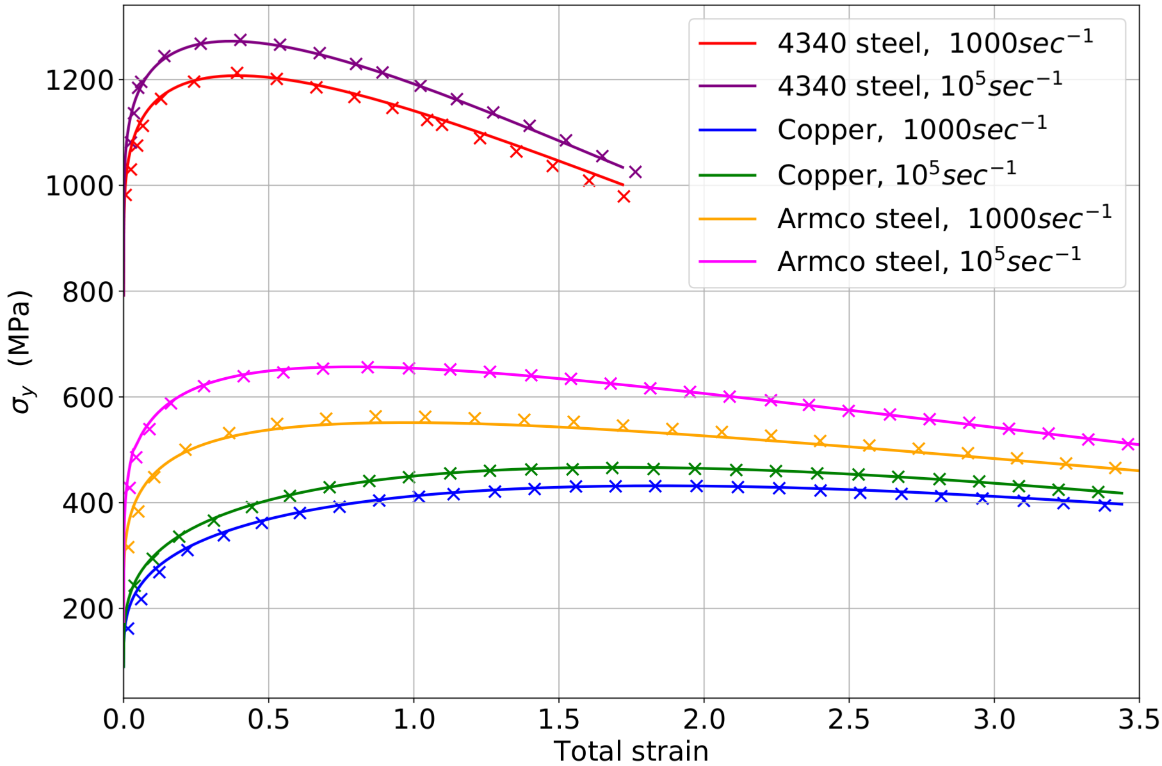

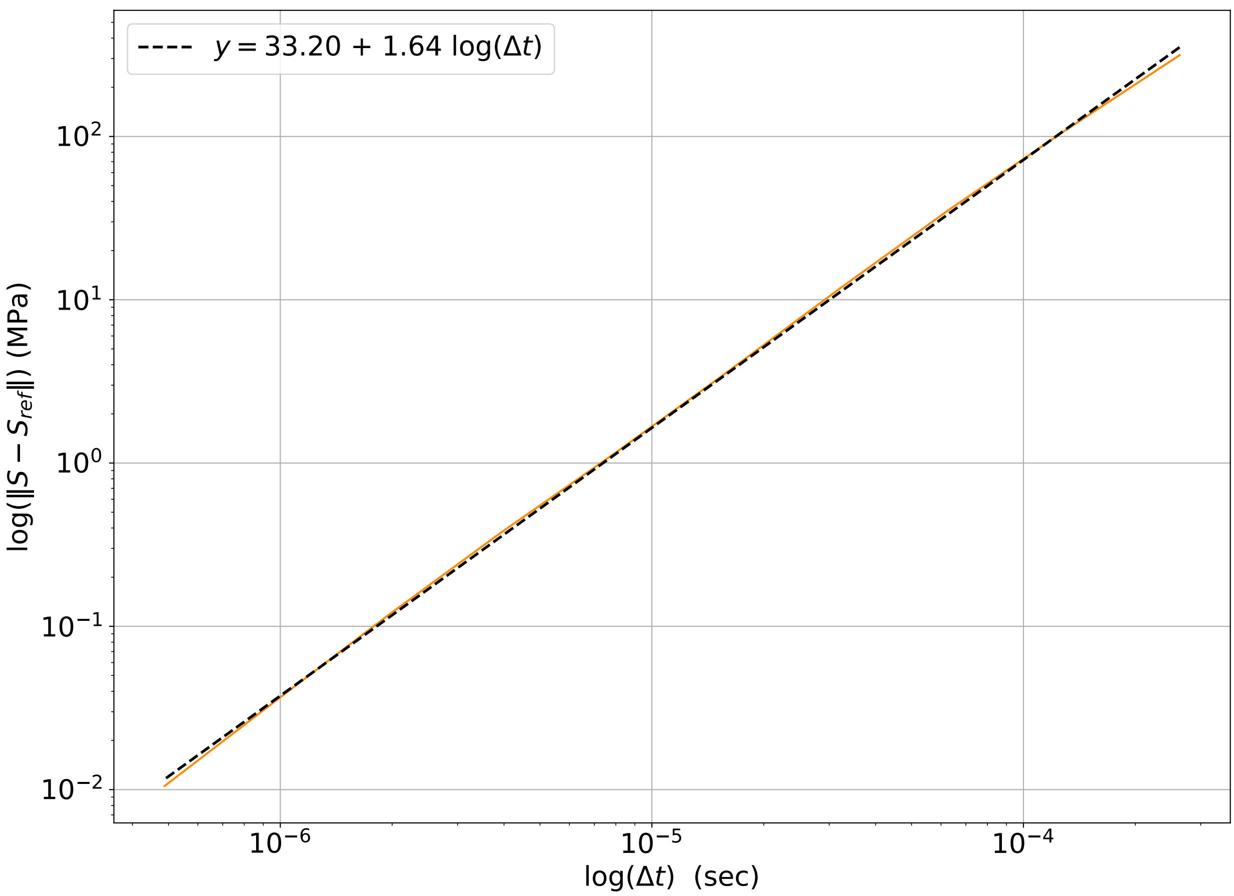

Examples

Collapse of a 2D beryllium shell

- 2D beryllium shell with inner and outer radii of 0.08 and 0.1 m, respectively, and initial radial velocity $u_r = -147.1\frac{1}{r}$.
- We compare our numerical results against a novel semi-analytical solution

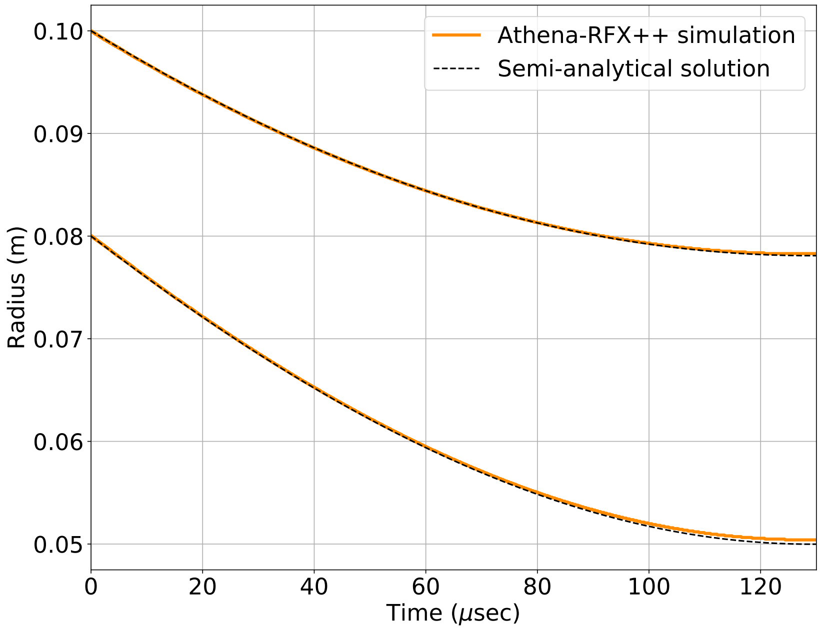

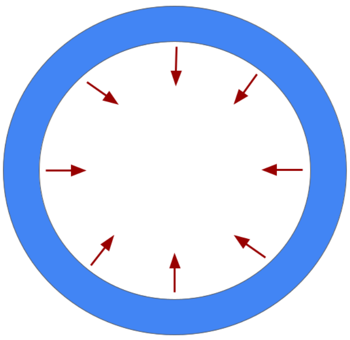

Taylor rod impact

- Cylindrical bar impacts a rigid wall with an initial velocity.
- Typically used for experimentally evaluating strength properties of materials.
- In the following examples, we compare our numerical simulations to experimental results from Konokman et al. (2011) [KÇK11].
- We consider results for aluminum (6061-T6) made bar with initial radius and length of 4.85 mm and 30 mm respectively.
- Johnson-Cook parameters from [LKL01]

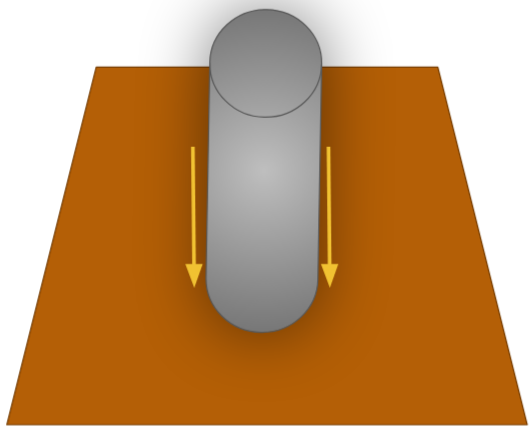

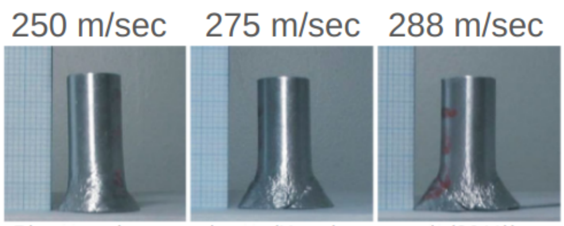

Photographs, experiment (Konokman et al. (2011))

Taylor rod impact

In the following figures, black dots are experimental points at final time from Konokman et al. (2011).

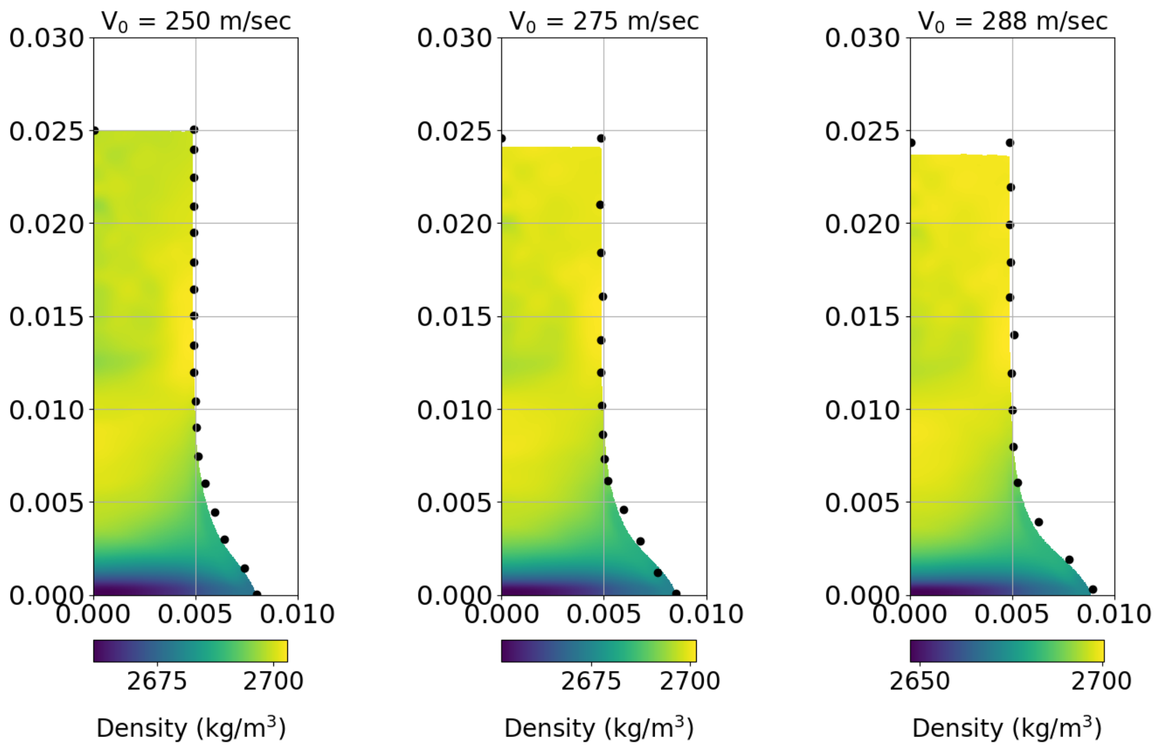

Copper jet

- In this problem, a copper jet is initiated by a shock wave that impacts a hemispherical groove.
- The elastic-plastic deforming material is conjugated with the surroundings air flow.
- Jet velocity and radius are influenced by the radius of the hemispherical groove.
- We consider four radii dimensions and compare our results against experimental data from Mali 1973 [Mal73] and computational results from Wallis et al. (2021) [WBN21].

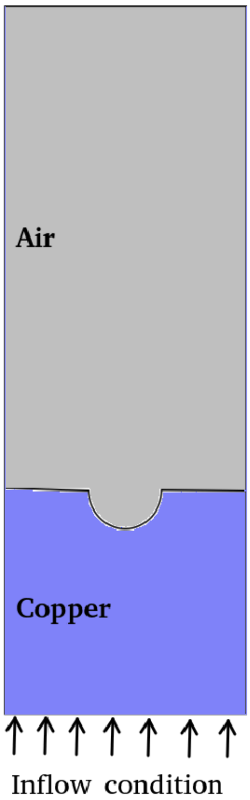

Copper jet

Velocity, temperature and density distributions at $t = 16$ μs for $R = 4$ mm.

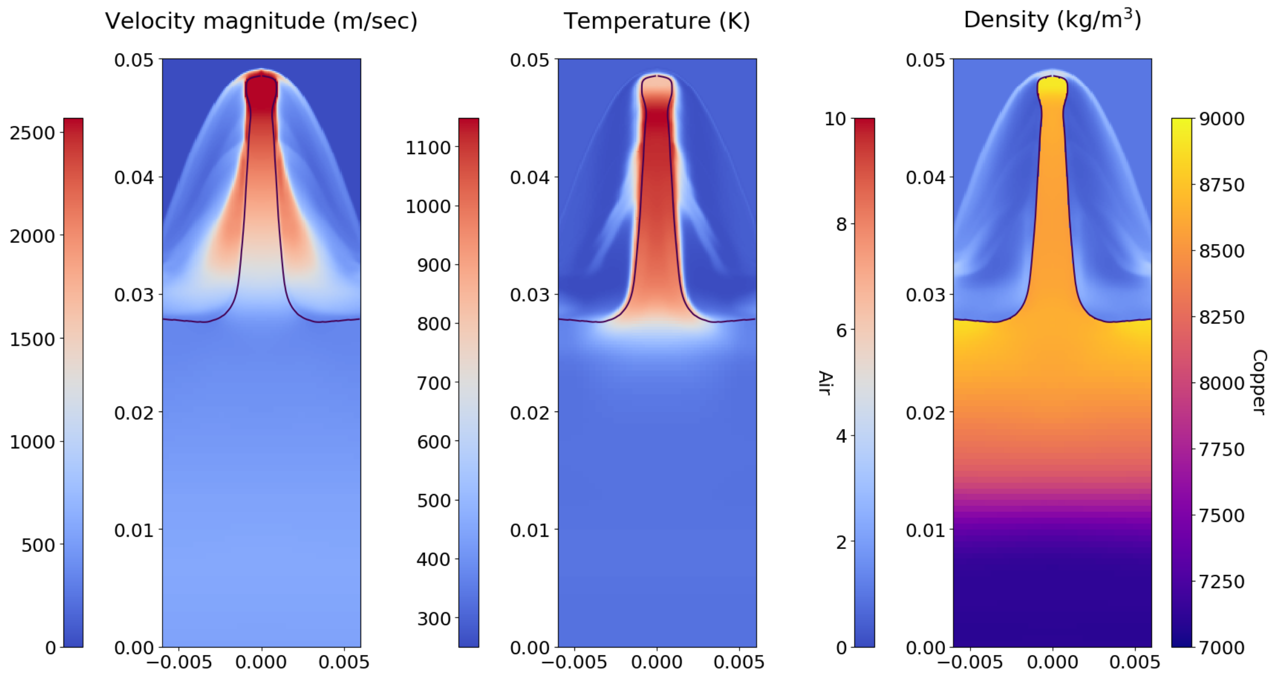

Copper jet

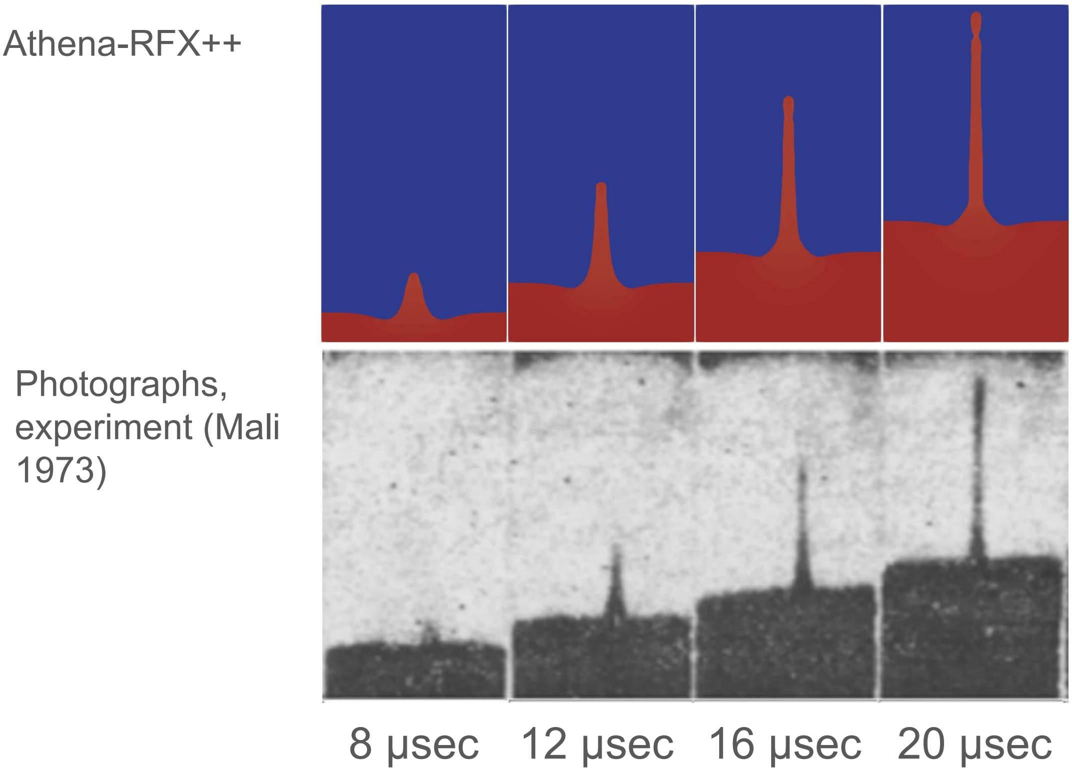

Copper jet

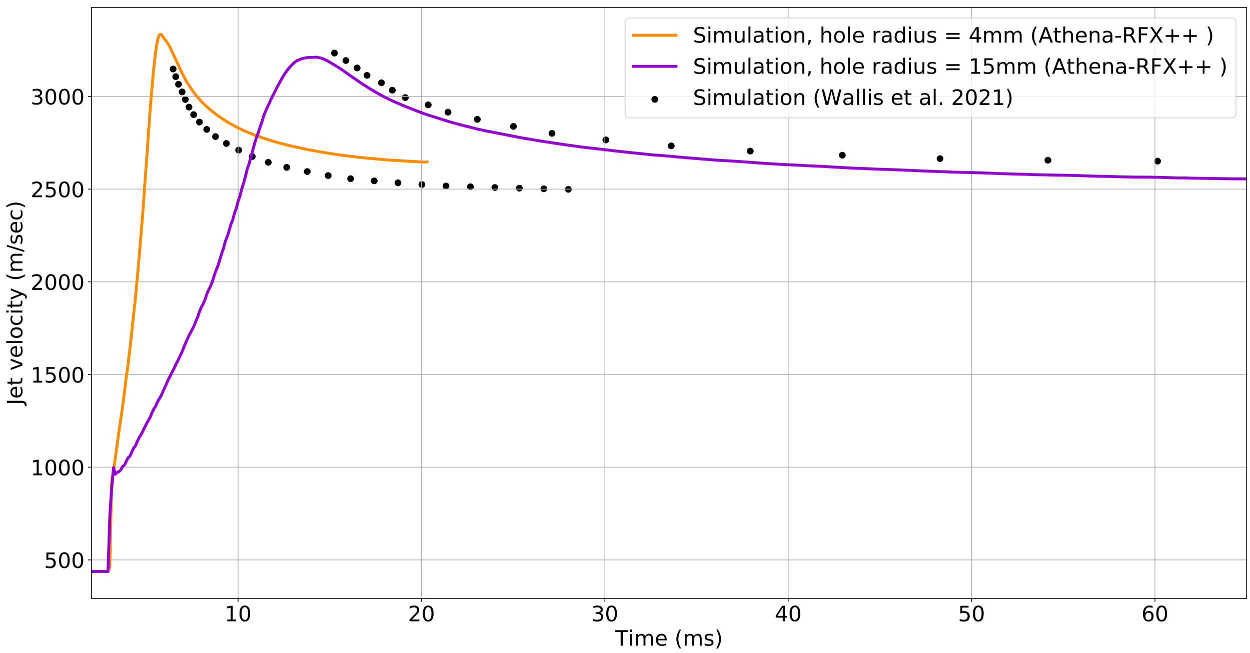

Copper jet

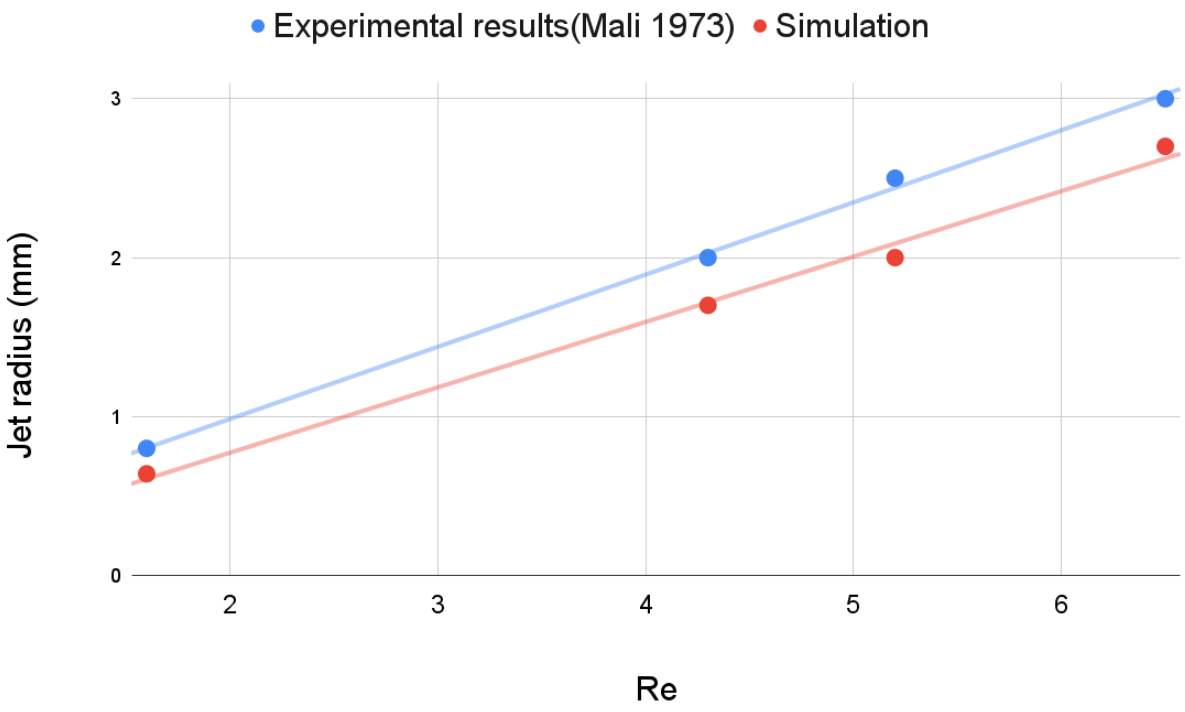

[1] Definition of *Re* can be found in Mali, 1973

Conclusion

- We developed a new 2D two-materials solver for the interaction of gas flow with elastic-plastic deformations of solid bodies.
- The new solver uses non-iterative procedure for elastic to plastic transition.
- We demonstrated the new solver capabilities by solving three benchmark problems and compared the solutions to reference and analytical solutions from the literature.
- Future work to do:
  1. Visco-elastic-plastic model
  2. Inclusion of penetration problems
  3. High-order temporal accuracy.

Thank you for your attention!

[1] We would like to thank the Israel Innovation Authority and MAFAT for funding this research.

References

- Gordon R Johnson and William H Cook, *Fracture characteristics of three metals subjected to various strains, strain rates, temperatures and pressures*, Engineering fracture mechanics **21** (1985), no. 1, 31–48.
- H Emrah Konokman, M Murat Çoruh, and Altan Kayran, *Computational and experimental study of high-speed impact of metallic taylor cylinders*, Acta mechanica **220** (2011), 61–85.
- Donald R Lesuer, GJ Kay, and MM LeBlanc, *Modeling large-strain, high-rate deformation in metals*, Tech. report, Lawrence Livermore National Lab.(LLNL), Livermore, CA (United States), 2001.
- VI Mali, *Flow of metals with a hemispherical indentation under the action of shock waves*, Combustion, Explosion and Shock Waves **9** (1973), no. 2, 241–245.
- Mark L Wilkins et al., *Calculation of elastic-plastic flow*, University of California, Ernest L. Lawrence Radiation Laboratory . . . , 1963.
- Tim Wallis, Philip T Barton, and Nikolaos Nikiforakis, *A diffuse interface model of reactive-fluids and solid-dynamics*, Computers & Structures **254** (2021), 106578.